Surface tension and curvature energy of quark matter in the Nambu–Jona-Lasinio model

G. Lugones,[1] A. G. Grunfeld,[2,3] and M. Al Ajmi[4]

[1]*Universidade Federal do ABC, Rua Santa Adélia, 166, 09210-170 Santo André, Brazil*

[2]*CONICET, Rivadavia 1917, 1033 Buenos Aires, Argentina*

[3]*Departamento de Física, Comisión Nacional de Energía Atómica, 1429 Buenos Aires, Argentina*

[4]*Department of Physics, Sultan Qaboos University, P.O. Box 36 Al-Khode 123, Muscat, Sultanate of Oman*

In this article we study the surface tension and the curvature energy of three-flavor quark matter in equilibrium under weak interactions within the Nambu–Jona-Lasinio model. We include the effect of color superconductivity and describe finite size effects within the multiple reflection expansion framework. Our calculations result in large values of the surface tension which disfavor the formation of mixed phases at the hadron-quark interphase inside a hybrid star.

I. INTRODUCTION

The study of the surface tension of deconfined quark matter has attracted much attention recently [1–4] because a detailed knowledge of it may contribute to a better comprehension of the physics of compact star interiors. In fact, surface tension plays a crucial role in quark matter nucleation during the formation of compact stellar objects, because it determines the nucleation rate and the associated critical size of the nucleated drops [5,6]. It is also determinant in the formation of mixed phases at the core of hybrid stars which may arise only if the surface tension is smaller than a critical value of the order of tens of MeV/fm^2 [7–10]. Also, surface tension affects decisively the properties of the most external layers of a strange star which may fragment into a charge-separated mixture, involving positively charged strangelets immersed in a negatively charged sea of electrons, presumably forming a crystalline solid crust [11]. This would happen below a critical surface tension which is typically of the order of a few MeV/fm^2 [12].

However, in spite of its key role in compact star physics, the surface tension is still poorly known for quark matter. Early calculations by Berger and Jaffe gave rather low values for the surface tension, below 5 MeV/fm^2 [13]. However, larger values within 10–50 MeV/fm^2 were used in other works about quark matter droplets in neutron stars [14,15]. More recently, values around ≈30 MeV/fm^2 have been adopted for studying the effect of quark matter nucleation on the evolution of protoneutron stars [16,17]. However, much larger values have also been obtained in the literature. Estimates given in Ref. [7] give values in the range 50–150 MeV/fm^2 and values around ∼300 MeV/fm^2 were suggested on the basis of dimensional analysis of the minimal interface between a color-flavor locked phase and nuclear matter [18].

In this article we study the surface tension and the curvature energy of three-flavor quark matter in equilibrium under weak interactions within the Nambu–Jona-Lasinio (NJL) model. We include the effect of color superconductivity and describe finite size effects within the multiple reflection expansion (MRE) framework [19–22]. We consider only the two-flavor color superconducting (2SC) phase, but we see that our conclusions are quite general and the results for other superconducting

phases can be easily foreseen within the present model. Our calculations result in large values of the surface tension which disfavor the formation of mixed phases at hybrid star cores.

The article is organized as follows: in Sec. II we present the quark matter equations of state without finite size effects. Then, in Sec. III we introduce the MRE formalism for the finite size effects. Finally, in Sec. IV we present our results and conclusions.

II. THE MODEL IN THE BULK

In the present work we start from an SU(3)$_f$ NJL effective model which also includes color superconducting quark-quark interactions. The corresponding Lagrangian is given by

$$\mathcal{L} = \bar{\psi}(i/\!\!\!\partial - \hat{m})\psi + G \sum_{a=0}^{8}[(\bar{\psi}\,\tau_a\,\psi)^2 + (\bar{\psi}\,i\gamma_5\tau_a\,\psi)^2]$$
$$+ 2H \sum_{A,A'=2,5,7}[(\bar{\psi}\,i\gamma_5\tau_A\lambda_{A'}\,\psi_C)(\bar{\psi}_C\,i\gamma_5\tau_A\lambda_{A'}\,\psi)], \quad (1)$$

where $\hat{m} = \text{diag}(m_u, m_d, m_s)$ is the current mass matrix in flavor space. In what follows we work in the isospin symmetric limit $m_u = m_d = m$, and for simplicity we do not include flavor mixing effects. The matrices τ_i and λ_i with $i = 1, \ldots, 8$ are the Gell-Mann matrices corresponding to the flavor and color groups, respectively, and $\tau_0 = \sqrt{2/3}\,1_f$. In addition, in Eq. (1) we used the charge conjugate spinors $\psi_C = C\bar{\psi}^T$ and $\bar{\psi}_C = \psi^T C$, where $\bar{\psi} = \psi^\dagger\gamma^0$ is the Dirac conjugate spinor and $C = i\gamma^2\gamma^0$.

The next step is obtaining the grand canonical thermodynamic potential at finite temperature T and chemical potentials μ_{fc}, where f and c stand for flavor and color, respectively. Then, we are able to calculate the relevant thermodynamic quantities. Note that first we show the thermodynamic potential for the bulk system, and later on we derive the effective potential for the finite size effects. For that purpose, starting from Eq. (1), it is convenient to perform a standard bosonization of the theory. Thus, we introduce the bosonic fields σ_a, π_a, and Δ_A corresponding to the sigma and pion mesons, and scalar diquark fields, respectively, and integrate

out the quark fields. In what follows we work within the mean field approximation (MFA), in which these bosonic fields are expanded around their vacuum expectation values and the corresponding fluctuations are neglected. Since the mean field values of the pion fields vanish due to symmetry reasons, in what follows we only consider those of the sigma and diquark fields. Then, $\hat{\sigma} = \sigma_a \tau_a = \text{diag}(\sigma_u, \sigma_d, \sigma_s)$ and $\pi_a = 0$. Regarding the diquark mean field, in the present work we assume that in the density region of interest only the 2SC phase might be relevant. Moreover, because of the color symmetry, one can rotate in color space to fix $\Delta_5 = \Delta_7 = 0$, $\Delta_2 = \Delta$. Finally, in the framework of the Matsubara and Nambu-Gorkov formalism we obtain the following MFA thermodynamic potential $\Omega_{\text{MFA}}(T, \mu_{fc}, \sigma_u, \sigma_d, \sigma_s, |\Delta|)$ per unit volume (further calculation details can be found in Refs. [23–30]):

$$\frac{\Omega_{\text{MFA}}}{V} = 2 \int_0^\Lambda \frac{k^2 dk}{2\pi^2} \sum_{i=1}^9 \omega(x_i, y_i)$$
$$+ \frac{1}{4G}(\sigma_u^2 + \sigma_d^2 + \sigma_s^2) + \frac{|\Delta|^2}{2H}, \quad (2)$$

where Λ is the cutoff of the model and $\omega(x, y)$ is defined by

$$\omega(x, y) = -x - T \ln[1 + e^{-(x-y)/T}]$$
$$- T \ln[1 + e^{-(x+y)/T}], \quad (3)$$

with

$$x_{1,2} = E, \quad x_{3,4,5} = E_s, \quad (4)$$
$$x_{6,7} = ([E \pm (\mu_{ur} + \mu_{dg})/2]^2 + \Delta^2)^{1/2}, \quad (5)$$
$$x_{8,9} = ([E \pm (\mu_{ug} + \mu_{dr})/2]^2 + \Delta^2)^{1/2}, \quad (6)$$
$$y_1 = \mu_{ub}, \quad y_2 = \mu_{db}, \quad y_3 = \mu_{sr}, \quad (7)$$
$$y_4 = \mu_{sg}, \quad y_5 = \mu_{sb}, \quad (8)$$
$$y_{6,7} = (\mu_{ur} - \mu_{dg})/2, \quad y_{8,9} = (\mu_{ug} - \mu_{dr})/2. \quad (9)$$

In the above expressions $E = \sqrt{k^2 + M^2}$ and $E_s = \sqrt{k^2 + M_s^2}$, with $M_f = m_f + \sigma_f$. Because we are working in the isospin limit, $\sigma_u = \sigma_d = \sigma$, which gives $M_u = M_d = M$. In principle one has nine different quark chemical potentials, corresponding to the three quark flavors (u, d, and s) and three quark colors (r, g, and b). Nevertheless, as discussed above, with our particular election of the orientation of the gap Δ in the color space, there is a residual color symmetry (between red and green colors). Moreover, if we require the system to be in chemical equilibrium, it can be seen that all chemical potentials are not independent from each other, as discussed in the next section.

The total thermodynamic potential is obtained by adding to Ω_{MFA} the contribution of the electrons and a vacuum constant. Namely,

$$\Omega = \Omega_{\text{MFA}} + \Omega_e - \Omega_{\text{vac}}, \quad (10)$$

where Ω_e is the thermodynamic potential of the electrons. For them we use the expression corresponding to a free gas of ultrarelativistic fermions,

$$\frac{\Omega_e(T, \mu_e)}{V} = -2\left(\frac{\mu_e^4}{24\pi^2} + \frac{\mu_e^2 T^2}{12} + \frac{7\pi^2 T^4}{360}\right). \quad (11)$$

It is important to notice that in Eq. (10) we have subtracted the constant $\Omega_{\text{vac}} \equiv -P_{\text{vac}} V$ in order to have a vanishing pressure at vanishing temperature and chemical potentials. However, this conventional prescription is merely an arbitrary way to uniquely determine the equation of state (EOS) of the NJL model without any further assumptions [31]. In the MIT bag model for instance, the pressure in the vacuum is nonvanishing. In view of this, Ω_{vac} is taken as a free parameter in Ref. [31], having in mind that tuning this constant is an easy way to control the splitting between the chiral restoration density and the deconfinement density. Nevertheless, we see below that Ω_{vac} does not have a direct influence on the values of the surface tension and the curvature energy.

III. FINITE SIZE EFFECTS

A. MRE formalism

Now we are ready to introduce the effects of finite size in the thermodynamic potential. For doing so we consider the multiple reflection expansion formalism (see Refs. [19–22] and references therein), which consists of modifying the density of states for the case of a finite spherical droplet as follows:

$$\rho_{\text{MRE}}(k, m_f, R) = 1 + \frac{6\pi^2}{kR} f_S + \frac{12\pi^2}{(kR)^2} f_C, \quad (12)$$

where the surface contribution to the density of states is

$$f_S = -\frac{1}{8\pi}\left(1 - \frac{2}{\pi} \arctan \frac{k}{m_f}\right), \quad (13)$$

and the curvature contribution is given in the Madsen ansatz [20]

$$f_C = \frac{1}{12\pi^2}\left[1 - \frac{3k}{2m_f}\left(\frac{\pi}{2} - \arctan \frac{k}{m_f}\right)\right] \quad (14)$$

to take into account the finite quark mass contribution.

The density of states of MRE for massive quarks is reduced compared with the bulk one, and for a range of small momenta becomes negative. These nonphysical negative values are removed by introducing an infrared (IR) cutoff in momentum space [22]. Thus, we have to perform the following replacement in order to obtain the thermodynamic quantities:

$$\int_0^\Lambda \cdots \frac{k^2 dk}{2\pi^2} \longrightarrow \int_{\Lambda_{\text{IR}}}^\Lambda \cdots \frac{k^2 dk}{2\pi^2} \rho_{\text{MRE}}. \quad (15)$$

The IR cutoff Λ_{IR} is the largest solution of the equation $\rho_{\text{MRE}}(k) = 0$ with respect to the momentum k.

After the above replacement, the full thermodynamic potential for finite size spherical droplets reads

$$\frac{\Omega_{\text{MRE}}}{V} = 2 \int_{\Lambda_{IR}}^\Lambda \frac{k^2 dk}{2\pi^2} \rho_{\text{MRE}} \sum_{i=1}^9 \omega(x_i, y_i)$$
$$+ \frac{1}{4G}(\sigma_u^2 + \sigma_d^2 + \sigma_s^2) + \frac{|\Delta|^2}{2H} - P_e + P_{\text{vac}}. \quad (16)$$

Multiplying on both sides of the last equation by the volume of the quark matter drop and rearranging terms we arrive at

the following form for Ω_{MRE}:

$$\Omega_{\mathrm{MRE}} = -PV + \alpha S + \gamma C, \qquad (17)$$

where the pressure P, the surface tension, and the curvature energy density are defined as [6]

$$
\begin{aligned}
P &\equiv -\frac{\partial \Omega_{\mathrm{MRE}}}{\partial V}\bigg|_{T,\mu,S,C} \\
&= -2 \int_{\Lambda_{\mathrm{IR}}}^{\Lambda} \frac{k^2 dk}{2\pi^2} \sum_{i=1}^{9} \omega(x_i, y_i) - \frac{1}{4G}\left(\sigma_u^2 + \sigma_d^2 + \sigma_s^2\right) \\
&\quad - \frac{|\Delta|^2}{2H} + P_e - P_{\mathrm{vac}},
\end{aligned} \qquad (18)
$$

$$\alpha \equiv \frac{\partial \Omega_{\mathrm{MRE}}}{\partial S}\bigg|_{T,\mu,V,C} = 2 \int_{\Lambda_{\mathrm{IR}}}^{\Lambda} k\, dk\, f_S \sum_{i=1}^{9} \omega(x_i, y_i), \qquad (19)$$

and

$$\gamma \equiv \frac{\partial \Omega_{\mathrm{MRE}}}{\partial C}\bigg|_{T,\mu,V,S} = 2 \int_{\Lambda_{\mathrm{IR}}}^{\Lambda} dk\, f_C \sum_{i=1}^{9} \omega(x_i, y_i), \qquad (20)$$

respectively. We consider a spherical drop; i.e., the area is $S = 4\pi R^2$ and the curvature is $C = 8\pi R$.

As mentioned above, once we have the grand thermodynamic potential Ω_{MRE} then we can obtain the relevant thermodynamic quantities. We can readily obtain the number density of quarks of each flavor and color,

$$n_{fc} \equiv \frac{1}{V} \frac{\partial \Omega_{\mathrm{MRE}}}{\partial \mu_{fc}}, \qquad (21)$$

and the number density of e^- (assumed to be massless),

$$n_e \equiv \frac{1}{V} \frac{\partial \Omega_{\mathrm{MRE}}}{\partial \mu_e}. \qquad (22)$$

Then, the corresponding number densities of each flavor, n_f, and of each color, n_c, in the quark phase are given by $n_f = \sum_c n_{fc}$ and $n_c = \sum_f n_{fc}$, respectively. The baryon number density reads $n_B = \frac{1}{3} \sum_{fc} n_{fc} = (n_u + n_d + n_s)/3$.

B. Neutrality conditions and β decay

To derive the EOS from the above formalism it is necessary to impose a suitable number of conditions on the variables $\{\mu_{fc}\}, \mu_e, \sigma, \sigma_s,$ and Δ. The first three of these conditions arise from the fact that the thermodynamically consistent solutions correspond to the stationary points of Ω_{MRE} with respect to σ, σ_s, and Δ. Then, we have

$$\frac{\partial \Omega_{\mathrm{MRE}}}{\partial \sigma} = 0, \quad \frac{\partial \Omega_{\mathrm{MRE}}}{\partial \sigma_s} = 0, \quad \frac{\partial \Omega_{\mathrm{MRE}}}{\partial |\Delta|} = 0. \qquad (23)$$

For the remaining conditions one must specify the physical situation in which one is interested. In this work we are interested in the study of finite size color superconducting droplets in β equilibrium that may form, e.g., within the mixed phase of a hybrid star. In such a case, chemical equilibrium is maintained by weak interactions among quarks; e.g., $d \leftrightarrow u + e^- + \bar{\nu}_e$, $s \leftrightarrow u + e^- + \bar{\nu}_e$, $u + d \leftrightarrow u + s$. Here

we consider the situation of no neutrino trapping. Then, the lepton number is not conserved and we have four independent conserved charges, namely the electric charge $n_Q = \frac{2}{3}n_u - \frac{1}{3}n_d - \frac{1}{3}n_s - n_e$ and the three color charges $n_u, n_d,$ and n_s. It is more convenient to use the linear combinations $n = n_r + n_g + n_b$, $n_3 = n_r - n_g$, and $n_8 = \frac{1}{\sqrt{3}}(n_r + n_g - 2n_b)$, where $n = 3n_B$ (the total quark number density) and n_3 and n_8 are related with color asymmetries. Thus, conserved charges $\{n_j\} = \{n, n_3, n_8, n_Q\}$ are related to four independent chemical potentials $\{\mu_j\} = \{\mu, \mu_3, \mu_8, \mu_Q\}$ such that $n_j = -\partial \Omega_{\mathrm{MRE}}/\partial \mu_j$. The individual quark chemical potentials μ_{fc} are given by

$$
\begin{aligned}
\mu_{fc} = \mu &+ \mu_Q \left[\frac{1}{2}(\tau_3)_{ff} + \frac{1}{2\sqrt{3}}(\tau_8)_{ff}\right] \\
&+ \mu_3(\lambda_3)_{cc} + \mu_8(\lambda_8)_{cc},
\end{aligned} \qquad (24)
$$

where, as before, τ_i and λ_i are the Gell-Mann matrices in flavor and color space, respectively.

From the β-equilibrium conditions we have

$$\mu_{dc} = \mu_{sc} = \mu_{uc} + \mu_e \qquad (25)$$

for all colors c. Then, the electron chemical potential is $\mu_e = -\mu_Q$. Finally, the rest of the conditions we need to impose for electrically and color neutral matter are

$$n_Q \equiv -\frac{\partial \Omega}{\partial \mu_Q} = 0, \quad n_8 \equiv -\frac{\partial \Omega}{\partial \mu_8} = 0. \qquad (26)$$

(Note: Remember that we choose a particular orientation of the gap in the color space, which introduces the r-g symmetry. Thus, we trivially satisfy $n_3 = 0$, and then μ_3 is automatically equal to zero.)

In summary, in the case of neutron star quark matter without neutrino trapping, for each value of μ (or μ_B) and T one can find the values of $\sigma, \sigma_s, \Delta, \mu_e,$ and μ_8 by solving Eqs. (23) and (26) supplemented by Eq. (25). This allows us to obtain the quark matter EOS in the thermodynamic region of interest and we can evaluate the curvature energy and surface tension of the color superconducting droplets.

It is important to remark that, in general, when we numerically solve the set of equations related with all the conditions discussed above, there might be regions for which there is more than one solution for each value of T and μ. To choose the stable solution among all of them, we require it to be an overall minimum of the thermodynamic potential.

C. Parametrization

The set of parameters we use in the present work is the following (those in Ref. [29] but without 't Hooft interactions): $m_{u,d} = 5.5$ MeV, $m_s = 112.0$ MeV, $\Lambda = 602.3$ MeV, and $G\Lambda^2 = 4.638$. Moreover, we considered the ratio $H/G = 3/4$ obtained from Fierz transformations of the one-gluon exchange interactions.

Because we impose vanishing pressure at vanishing temperature and chemical potentials for Fermi momentum $k_F \to 0$ (when $R \to \infty$) [21], P_0 is the same as in the bulk case. For the set of parameters we used, we found $\Omega_{\mathrm{vac}}/V = -P_{\mathrm{vac}} = -4301$ MeV/fm^3. However, we emphasize that the values

of the surface tension α and the curvature energy γ are not changed by the choice of P_{vac}.

As we previously mentioned, the value of Λ_{IR} is the largest root when solving $\rho_{\text{MRE}} = 0$ with respect to k, depending on m_f and R. We find that these solutions can be fitted through the following rule:

$$\Lambda_{\text{IR}} = a \, R^b \tag{27}$$

with R in femtometers and Λ_{IR} in MeV. The coefficients for $m_u = 5.5$ MeV are $a = 135.45$ and $b = -0.85$. For $m_s = 112$ MeV we have $a = 228.60$ and $b = -0.87$.

IV. RESULTS AND CONCLUSIONS

In Fig. 1 we show our results for the surface tension α and curvature energy γ of the color superconducting droplets as a function of the quark chemical potential, for two different temperatures and four different radii. The temperatures 30 MeV and 5 MeV are representative, respectively, of the conditions prevailing at the beginning and at the end of the cooling or deleptonization phase of protoneutron star evolution. We checked that the results for $T = 5$ MeV are almost indistinguishable from those for zero temperature; thus, in practice they also represent old and cold neutron stars. We show results for drops with radii ranging from very small values of 5 fm, which have a large energy cost due to

surface and curvature effects, to the bulk limit of $R = \infty$. For given values of R, T, and μ there may exist more than one solution of the equations. If more than one solution is found, the one that minimizes the thermodynamic potential is chosen. As explained in the figure caption, the left-hand branches correspond to the chiral symmetry broken phase and the right-hand curves after the discontinuity to the 2SC phase. For the curves presenting negative pressures we introduced a dot indicating the zero pressure point. The part of the curve to the left of the dot corresponds to $P \leqslant 0$. Note that, as previously mentioned, we subtracted Ω_{vac} to have vanishing pressure at vanishing T and μ for $R = \infty$. However, Ω_{vac} can be taken as a free parameter as in Ref. [31]. In this case, the dot in the figures can move along the curves. However, it is clear from Eqs. (19) and (20) that a nonstandard choice for Ω_{vac} does not change the numerical values of α and γ for given R, T, and μ.

Our results show that the surface tension is in the range $\alpha \sim 145$–165 MeV/fm^2 and the curvature energy is in the range $\gamma \sim 95$–110 MeV/fm. The large values of the surface and curvature energies are due to the linear term in the expression for $\omega(x, y)$ in Eq. (3), which is not present in the thermodynamic potential of, e.g., the MIT bag model. For a given μ, the surface tension is an increasing function of R. The curvature energy behaves differently at constant μ: for very small radii (~ 5–10 fm) it increases with R, but in the range from 10 fm to ∞ it is a decreasing function of R.
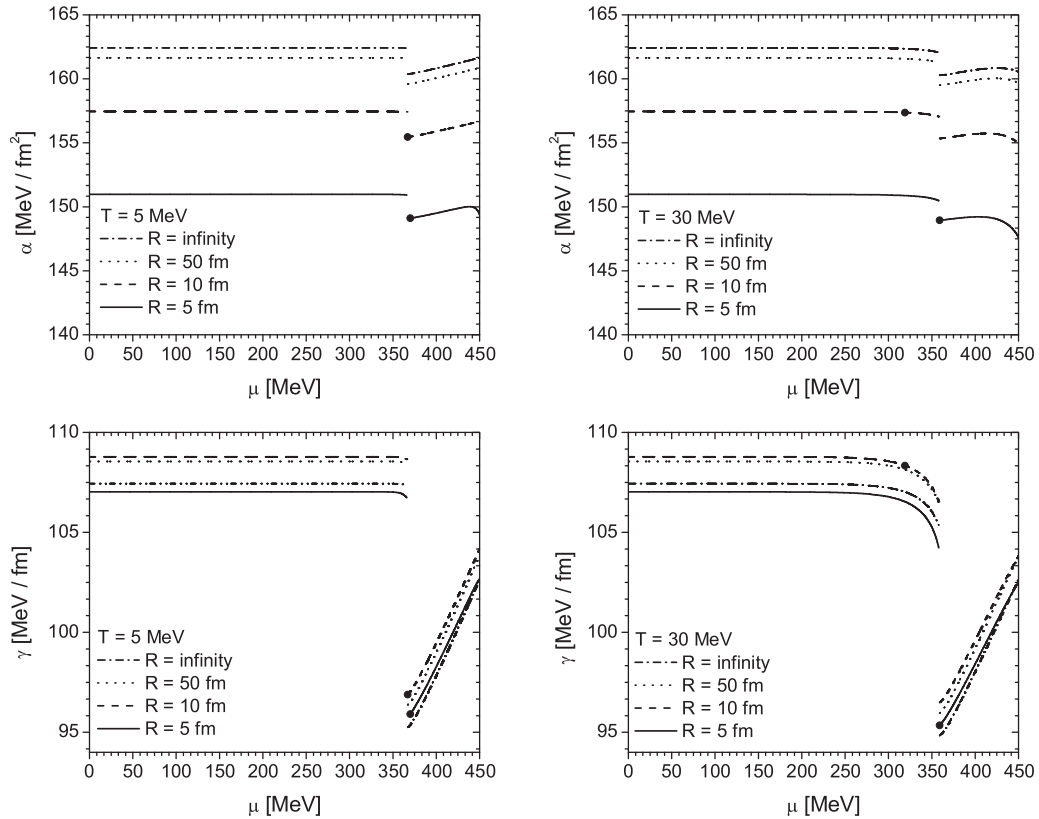

FIG. 1. Surface tension α and curvature energy γ for different radii and temperatures. In all panels, the left-hand branches correspond to the solutions in which the chiral symmetry broken phase is more favorable and the right-hand curves, after the discontinuity, correspond to the 2SC solutions.

Of course, both the surface and curvature contributions to the free energy per unit volume Ω_{MRE}/V tend to zero as $R \to \infty$, as can be checked from Eq. (17). The different behavior with R for α and γ is a consequence of the functional form of the integrand together with the R dependence of the IR cutoff. The integral for the surface tension has a fixed upper limit (the ultraviolet cutoff Λ), but the lower limit (Λ_{IR}) decreases with R. Then, as R increases, Λ_{IR} decreases, the area under the curve increases, and, as a result, the surface tension increases. For the curvature energy the effect is different. The integrand is positive for large k but negative for small k. For small R, Λ_{IR} falls in the positive region of the integrand. Thus, as Λ_{IR} decreases, the positive area under the curve increases, and the curvature energy increases. For larger R, Λ_{IR} falls in the negative region of the integrand. Consequently, as Λ_{IR} decreases, the negative part of the area under the curve increases, and the curvature energy decreases. The results in Fig. 1 show that the temperature dependence of α and γ is very weak for the values of T that are relevant for protoneutron stars and cold neutron stars. Note also that these results are of the same order as those obtained within the NJL model for just deconfined quark matter *out of chemical equilibrium* under weak interactions [5,6].

The present equation of state can support a two-solar-mass neutron star such as the pulsars PSR J1614-2230 [32] and PSR J0348-0432 [33] if a sufficiently stiff hadronic equation of state is employed for the outer layers of the star (see, for example, Fig. 4 of Ref. [31]). Adding a vector interaction to the NJL model, it is possible to stiffen the EOS and obtain larger stellar masses. The vector term affects the surface tension in a nontrivial way. The chemical potentials gain an extra term $\mu_{u,d,s} - 4g_v \langle \psi^\dagger \psi \rangle_{u,d,s}$ that shifts chemical equilibrium and the pressure gains a term proportional to the square of the density. The combined effect is difficult to estimate without a full calculation, which will be addressed in future work. According to recent work [34], within a geometric approach to the surface tension evaluation, the surface tension can be

lowered by the presence of a repulsive vector term and for magnetized quark matter the value is further lowered [35]. However, within the MRE formalism the behavior may be different and deserves further study.

The large values of α and γ have strong consequences for the physics of neutron star interiors, because the energy cost of forming quark drops within the mixed phase of hybrid stars would be very large. According to Ref. [7], beyond a limiting value of $\alpha \approx 65$ MeV/fm^2 the structure of the mixed phase becomes mechanically unstable and local charge neutrality is recovered. Therefore, our results indicate that the hadron-quark interphase within a hybrid star should be a sharp discontinuity.

The consequences of the large values of α and γ for the triggering of the deconfinement transition in neutron and protoneutron stars were studied in Refs. [5,6]. The main difference from the present study of the quark-hadron interphase is the condition of chemical equilibrium. The nucleation (deconfinement) of the first quark matter drop that triggers the conversion of the core of a hadronic star is driven by strong interactions and consequently it happens out of chemical equilibrium under weak interactions. As shown in Ref. [6] the nucleation of quark matter is possible during the protoneutron star phase even for large values of the surface tension, because large drops (with a size of hundreds of femtometers) may have a huge nucleation rate. These large drops are charge neutral because flavor is conserved during the deconfinement transition [6] and therefore they can be considerably larger than the Debye screening length λ_D of the stellar plasma, which is typically 5–10 fm. Since these drops can be very large ($R \gtrsim 200$ fm [5,6]), surface and curvature effects tend to vanish. This is not the case for droplets of quark matter in the hypothetical mixed phase of a hybrid star. Because they are electrically charged their size cannot exceed $\sim \lambda_D$ (i.e., few femtometers) and therefore surface and curvature have a significant energy cost, inhibiting the formation of the mixed phase.

[1] M. Buballa and S. Carignano, Phys. Rev. D **87**, 054004 (2013).

[2] M. B. Pinto, V. Koch, and J. Randrup, Phys. Rev. C **86**, 025203 (2012).

[3] X. J. Wen, J. Y. Li, J. Q. Liang, and G. X. Peng, Phys. Rev. C **82**, 025809 (2010).

[4] L. F. Palhares and E. S. Fraga, Phys. Rev. D **82**, 125018 (2010).

[5] T. A. S. do Carmo, G. Lugones, and A. G. Grunfeld, J. Phys. G: Nucl. Part. Phys. **40**, 035201 (2013).

[6] G. Lugones and A. G. Grunfeld, Phys. Rev. D **84**, 085003 (2011).

[7] D. N. Voskresensky, M. Yasuhira, and T. Tatsumi, Nucl. Phys. A **723**, 291 (2003).

[8] T. Tatsumi, M. Yasuhira, and D. N. Voskresensky, Nucl. Phys. A **718**, 359 (2003).

[9] T. Maruyama, S. Chiba, H.-J. Schulze, and T. Tatsumi, Phys. Rev. D **76**, 123015 (2007).

[10] T. Endo, Phys. Rev. C **83**, 068801 (2011).

[11] P. Jaikumar, S. Reddy, and A. W. Steiner, Phys. Rev. Lett. **96**, 041101 (2006).

[12] M. G. Alford, K. Rajagopal, S. Reddy, and A. W. Steiner, Phys. Rev. D **73**, 114016 (2006).

[13] M. S. Berger and R. L. Jaffe, Phys. Rev. C **35**, 213 (1987); **44**, R566 (1991).

[14] H. Heiselberg, C. J. Pethick, and E. F. Staubo, Phys. Rev. Lett. **70**, 1355 (1993).

[15] K. Iida and K. Sato, Phys. Rev. C **58**, 2538 (1998).

[16] I. Bombaci, G. Lugones, and I. Vidaña, Astron. Astrophys. **462**, 1017 (2007).

[17] I. Bombaci, D. Logoteta, P. K. Panda, C. Providencia, and I. Vidana, Phys. Lett. B **680**, 448 (2009).

[18] M. G. Alford, K. Rajagopal, S. Reddy, and F. Wilczek, Phys. Rev. D **64**, 074017 (2001).

[19] R. Balian and C. Bloch, Ann. Phys. **60**, 401 (1970).

[20] J. Madsen, Phys. Rev. D **50**, 3328 (1994).

[21] O. Kiriyama and A. Hosaka, Phys. Rev. D **67**, 085010 (2003).

[22] O. Kiriyama, Phys. Rev. D **72**, 054009 (2005).

[23] M. Huang, P. F. Zhuang, and W. F. Chao, Phys. Rev. D **67**, 065015 (2003).

[24] S. B. Rüster, V. Werth, M. Buballa, I. A. Shovkovy, and D. H. Rischke, Phys. Rev. D **72**, 034004 (2005).

[25] D. Blaschke, S. Fredriksson, H. Grigorian, A. M. Oztas, and F. Sandin, Phys. Rev. D **72**, 065020 (2005).

[26] H. Abuki, M. Kitazawa, and T. Kunihiro, Phys. Lett. B **615**, 102 (2005).

[27] H. Abuki and T. Kunihiro, Nucl. Phys. A **768**, 118 (2006).

[28] M. Ciminale, R. Gatto, N. D. Ippolito, G. Nardulli, and M. Ruggieri, Phys. Rev. D **77**, 054023 (2008).

[29] T. Hatsuda and T. Kunihiro, Phys. Rept. **247**, 221 (1994).

[30] M. Buballa, Phys. Rept. **407**, 205 (2005).

[31] C. H. Lenzi and G. Lugones, Astrophys. J. **759**, 57 (2012).

[32] P. B. Demorest, T. Pennucci, S. M. Ransom, M. S. E. Roberts, and J. W. T. Hessels, Nature (London) **467**, 1081 (2010).

[33] J. Antoniadis *et al.*, Science **340**, 6131 (2013).

[34] A. F. Garcia and M. B. Pinto, Phys. Rev. C **88**, 025207 (2013).

[35] R. Z. Denke and M. B. Pinto, Phys. Rev. D **88**, 056008 (2013).